JURNAL KIMIA VALENSI
p-ISSN: 2460-6065; e-ISSN: 2548-3013
Journal homepage: https://journal.uinjkt.ac.id/index.php/valensi
Research Article

Component Discrimination and Anti-skin-aging Potency of Emprit and Red Ginger Essential Oil: Chemometric, Molecular Docking and Molecular Dynamics Study

Badrunanto[1], Shadila Fira Asoka[1], Wulan Tri Wahyuni[1,3], Muhammad Farid[1], Setyanto Tri Wahyudi[2,3], and Irmanida Batubara[1,3,*]

[1]*Department of Chemistry, Faculty of Mathematics and Natural Sciences, IPB University, Bogor (16680), Indonesia*
[2]*Department of Physics, Faculty of Mathematics and Natural Sciences, IPB University, Bogor (16680), Indonesia*
[3]*Tropical Biopharmaca Research Center, Institute of Research and Community Services, IPB University, Bogor (16128), Indonesia*

Email: ime@apps.ipb.ac.id

Article Info
Received: June 9, 2023
Revised: August 30, 2023
Accepted: October 15, 2023
Online: November 15, 2023

Citation:
Badrunanto, Asoka, S. F., Wahyuni, W. T., Farid, M., Wahyudi, S. T., & Batubara, I. (2023). Component Discrimination and Anti-skin-aging Potency of Emprit and Red Ginger Essential Oil: Chemometric, Molecular Docking and Molecular Dynamics Study. *Jurnal Kimia Valensi*, 9(2), 183–194.

Doi: 10.15408/jkv.v9i2.32765

Abstract

Emprit and red ginger essential oils (EOs) are natural sources of antioxidants that have the potential to be used in cosmetics, one of which is as an anti-skin-aging. The aim of this study was to determine the component differences and anti-skin-aging potential of the two EOs. The components were determined by GC-MS, while discrimination was done by chemometric. The potential of the components as the anti-skin-aging were evaluated by molecular docking and molecular dynamics (MD) simulations. A total 66 components were identified in both EOs, where eucalyptol (17.92%) and camphene (15.12%) were the main component in emprit and red ginger, respectively. Chemometric analysis revealed two discriminant clusters highlighting their dissimilarity with germacrene D and α-zingiberene are the key markers for differentiation. The docking and MD simulations were demonstrated the four main components of emprit EO, namely α-curcumene, α-zingiberene, β-bisabolene and β-sesquiphellandrene, have the best docking scores and interact with the enzymes with a relatively stable interaction. AdmetSAR evaluation of the four components has shown good bioavailability and declared safe. This study succeeded in revealing two ginger EOs differences based on their components and demonstrated the emprit ginger EO was more promising as a natural anti-skin-aging agent for further research.

Keywords: Anti-skin-aging, discrimination, emprit ginger, molecular docking, red ginger

1. INTRODUCTION

Emprit (Z. *officinale* var *amarum*) and red ginger (*Z. officinale* var *rubrum*) are two varieties of Indonesian ginger that are used for health purposes [1]. Ginger is usually used in various forms, one of which is essential oil (EO). The terpenes content in ginger EO was demonstrated to have several activities, including antioxidants [2]. An antioxidant is a substance which is able to prevent, inhibit, or delay the oxidation of the substrate due to oxidants, such as reactive oxygen species (ROS) and reactive nitrogen species (RNS) [3]. One of the health problems associated with the oxidation process is skin-aging. However, studies on the potential of emprit and red ginger EO as a natural anti-skin-aging are still limited.

Aging is the body's response to genetic programs and the progressive accumulated impact of human interaction with the environment. The aging is caused by several intrinsic factors, such as telomeres shortening and cellular metabolism, as well as extrinsic factors, such as UV radiation, pollutant and chemicals [4]. As the outermost part of the body, the skin is very susceptible to aging. Changes in characteristics such as wrinkling, dark spot, laxity and loss of elasticity are signs of skin-aging [5]. Intrinsic factors of skin-aging are mainly influenced by telomeres shortening accelerated by

ROS [6]. Meanwhile, extrinsic aging is mainly due to direct exposure to solar radiation, ROS production and triggering the activation of intrinsic factors leading to skin-aging [7].

The accumulation of the ROS also will trigger the activation of several enzymes related to the skin-aging such as hyaluronidase, collagenase, elastase and tyrosinase, resulting in skin dryness, wrinkles, elasticity loss and uneven pigmentation. Aging has also been associated with the involvement of advanced glycation end products (AGEs), which is a heterogeneous group of compounds resulting from a reaction of reducing sugars with proteins, lipids and nucleic acid through Maillard reaction [4]. AGEs are believed to play a role in aging, one of which is cause stiffness and skin elasticity loss in skin-aging [8]. Several components in natural ingredients were reported to exhibit anti-skin-aging activity by various mechanisms such as against ROS, AGEs or by inhibiting skin-aging-related enzymes [9,10]. One natural resource with the potential for use is ginger [11,12].

The ability of ginger to inhibit the skin-aging-related enzymes has been reported previously. Batubara et al. (2023) have reported the ability of the *Z. officinale* var *rubrum* EO to inhibit the tyrosinase enzyme [13]. While Feng *et al.* (2018) have demonstrated the ability of *Z. officinale* Roscoe EO to protect the skin from UVB and photoaging [14]. Meanwhile, other research has revealed the potential of the ethanol extract of three Indonesian ginger as anti-skin aging through in silico study [15]. Although the EO compositions of emprit and red ginger has been widely known, studies that reveal differences in components, key markers, anti-skin-aging potency and which variety is the best as a natural anti-skin-aging agent have not been reported. Preliminary information regarding this information is needed before conducting research in a wet laboratory. For this reason, computational-based studies, including chemometrics and molecular docking study followed by molecular dynamic simulations, could be used [15–17]. Our study aims to characterize the EOs from emprit and red ginger based on their components through chemometric analysis, namely principle component analysis (PCA) and heatmap with dendrogram. The differences in potential as anti-skin-aging were evaluated in this study by measuring the inhibitory strength of components on the skin-aging-related enzymes through molecular docking study and followed by molecular dynamics (MD) simulations to study the stability and interactions of protein-ligand complexes.

2. RESEARCH METHODS

Plant materials

The fresh rhizomes of *Z. officinale* var *amarum* and *Z. officinale* var *rubrum* were collected from the same agriculture area, namely South Nagrak village, Sukabumi regency, West Java province (6°52'16"S 106°48'17"E) with an altitude ± 485 masl. The cleaned rhizomes were then distilled for eight hours by hydrodistillation with a cohobating system to collect the oil. The ginger EO was separated from water, then dried over anhydrous sodium sulfate, stored in glass vials and placed in the freezer (4 ˚C) until further analysis.

GC-MS analysis

The component of ginger EOs were analyzed with a GC-MS system (Agilent 7890B, Agilent Technologies, Santa Clara, CA, USA). Firstly, EO were diluted in ethanol to make a 1% solution. The solution are injected into a GC-MS system with a 1.5:1 split mode ratio and run on an HP-5MS capillary column (30 m × 250 μm × 0.25 μm), UI 5% phenyl methyl siloxane (Agilent Technologies, Santa Clara, CA, USA). The GC oven conditions were the following: the initial temperature was held for 1 minute at 40 ˚C, then continued with 10 ˚C/min to 300 ˚C temperature program and a final hold was 4 min. The mass spectrometer (Agilent 5977A, Agilent Technologies, Santa Clara, CA, USA) settings were: 230 ˚C source temperature, 150 ˚C MS Quad temperature and 70 eV ionization energy. The helium was used as carrier gas with 1 mL/min flow rate. The mass range of compounds was scanned between 30 to 600 amu. Identification of the EO compounds was based on computer matching of mass spectra results against the mass spectra of known compounds in the NIST 17 library (USA National Institute of Science and Technology software, NIST, Gaithersburg, MD, USA).

Chemometric analysis

Discrimination of the two ginger EO components was done using MetaboAnalyst 5.0, available online at https://www.metaboanalyst.ca/. The PCA and Heatmap with dendrogram were used to comprehend the similar chemical constituents among the EOs [15]. Heatmap was created using the Euclidean distance measure and Ward's method for linkage analysis.

Table 1. Protein targets and molecular docking parameters

Protein	PDB ID	Native ligand	Grid box coordinates			Grid box Size	Conformer generated
			Center_x	Center_y	Center_z		
Hyaluronidase	2PE4	ACT	41.877	-22.142	-16.287	20	9
Collagenase	2TCL	RO4	73.986	8.655	9.279	20	9
Elastase	3F19	HS6	-11.338	-4.481	-18.305	20	9
Tyrosinase	5M8R	MMS	-30.322	-4.944	-24.773	20	9

In silico and molecular docking studies

All identified compounds from ginger EOs by GC-MS analysis were used as ligands to inhibit the corresponding protein's activity in the aging process, while ascorbic acid was used as the control ligand. The 3D structure of the ligands was obtained from https://pubchem.ncbi.nlm.nih.gov in ".sdf" format, then the geometry was optimized using ORCA (version 4.2.0) and converted to .pdb format. Crystallographic 3D protein structures were obtained from the RCSB protein data bank (http://www.rscb.org). Docking parameters used, such as exhaustiveness, grid box coordinates and size, were validated by re-docking using native ligand (**Table 1**). The re-docking conformation then overlapped with the experimental conformation and its root means square deviation (RMSD) was calculated. Parameters whose RMSD is less than 2 Å were used to simulate the studied ligands. Details of docking parameters are listed in **Table 1**. Ligand and protein structures were prepared as a target using Autodock Tools (version 1.5.7) by removing water molecules, metal atoms, the co-crystalized ligands and other non-covalent bonded molecules. Optimized protein structures were saved in .pdbqt format and molecular docking simulation was performed using Autodock Vina [18]. The docked ligand-receptor complex interaction simulation results are expressed as affinity energy ΔG (kcal/mol) and inhibition constants (K_i) were obtained using the equation $K_i = \exp(\Delta G/RT)$, where R is the gas constant (1.985×10^{-3} kcal/mol.K) and T is the room temperature (298.15 K). While for 3D and 2D visualization of selected ligand-receptor interactions, Biovia Discovery Studio Visualizer (version 21.1.0.20298) software was used.

MD simulation

MD simulations of the best protein-ligand complexes were performed using nanoscale molecular dynamics (NAMD) package [19,20]. Docked complex topologies are prepared using CHARMM-GUI (http://www.charmm-gui.org) [21]. In order to neutralize the system, 0.15 M ions (Na^+ and Cl^-) were added to the 10 Å water molecule dissolution box. System energy was minimized to obtain the lowest energy configuration and followed by equilibration for 10 ns before a production run of 1000 frames at 303.15 K, a temperature relevant to the optimum condition for enzymes in biological system, using the CHARMM36 force field. The isothermal–isobaric (NPT) ensemble was set to all MD simulation with periodic boundary conditions. After simulation, trajectory analysis such as root-mean square deviation (RMSD), root-mean square fluctuation (RMSF) and solvent-accessible surface area (SASA) were performed using VMD [22].

Absorption-distribution-metabolism-excretion-toxicity (ADMET) properties analysis

AdmetSAR analysis was tested in this study to evaluate the toxicity of the best ligands by using Lipinski filtering tools which is available online at http:lmmd.ecust.edu.cn/admetSAR2/ [23]. Advance predict level was applied for the predicting important descriptors of drug-likeness.

3. RESULTS AND DISCUSSION

Yield and composition of the EO

Sixty-six compounds were identified in EOs of two varieties of Indonesian ginger by the GC/MS analysis (**Table 2**). **Figure 1** showed the chromatogram differences of those EO. Yield of the EO from RG rhizome was higher (1.43%) than EG (1.21%). The yield differences of ginger EOs are influenced by several factors, including variety, geographical location and maturity stage [24]. Emprit ginger EO consists of 15 monoterpenes, 17 oxygenated monoterpenes, 22 sesquiterpenes and 6 oxygenated sesquiterpenes. Meanwhile, red ginger EO contains 47 components which consist of 12 monoterpenes, 20 oxygenated monoterpenes, 11 sesquiterpenes and 4 oxygenated sesquiterpenes. Several reported studies showed Indonesian ginger EOs have low levels of sesquiterpene, while monoterpene and oxygenated monoterpenes were higher [25,26]. In this study, sesquiterpene (36.67%) was the main component of EG, while the oxygenated monoterpene (42.55%) was the main component of RG. Eucalyptol was the main (17.92%) component in EG, while camphene is the main (15.12%) component in RG. High levels of camphene were also observed in our previous study on fresh red ginger essential oil, but with a combi-

Table 2. The main components of two Indonesian ginger EO analyzed by GC-MS

No.	RI	Components	Composition (%)		Similarity (%)
			Emprit ginger	Red ginger	
1	1013	(-)-α-Pinene	2.28±1.98[a]	1.13±1.95[a]	96
2	1014	(+)-α-Pinene	4.61±2.49[a]	3.48±1.63[a]	96
3	1024	Camphene	17.00±1.93[a]	15.12±1.23[a]	97
4	1046	β-Myrcene	1.22±0.08[a]	2.24±0.43[a]	96
5	1074	Eucalyptol	17.92±1.46[a]	12.59±0.24[b]	96
6	1110	Linalool	0.81±0.04[a]	1.10±0.59[a]	76
7	1141	Camphene hydrate	0.33±0.13[a]	-	97
8	1149	endo-Borneol	4.64±2.28[a]	3.30±1.99[a]	97
9	1159	(+)-α-Terpineol	1.42±0.45[a]	0.86±0.79[a]	91
10	1172	Citronellol	0.07±0.03[a]	1.73±1.14[a]	98
11	1179	Neral	2.71±1.03[a]	10.12±0.71[b]	95
12	1184	Geraniol	-	1.47±0.18[a]	95
13	1193	Citral	1.88±0.93[a]	12.70±6.79[a]	93
14	1285	α-Curcumene	2.96±0.51[a]	2.76±039[b]	98
15	1287	Germacrene D	1.16±0.09[a]	0.12±0.10[a]	99
16	1290	α-Zingiberene	13.30±1.49[a]	4.06±0.28[b]	95
17	1292	α-Farnesene	1.58±1.43[a]	0.77±0.69[a]	93
18	1295	β-Bisabolene	5.77±1.00[a]	2.21±0.41[b]	93
19	1302	β-Sesquiphellandrene	6.67±1.75[a]	2.25±0.33[b]	98

Note: RI= Retention indices. Data are shown as mean ± SD values, derived from three independent experiments. Means in the same row superscripted with different lowercase letters are significantly ($p < 0.05$) differently.

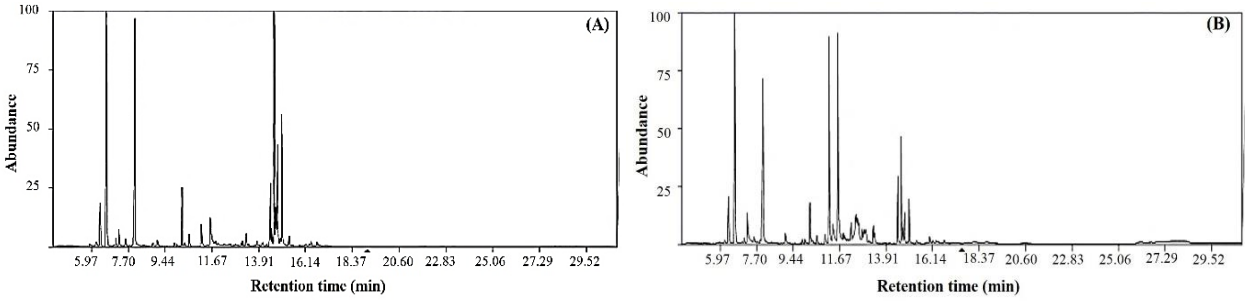

Figure 1. Chromatogram of (A) emprit ginger; (B) red ginger Eos

nation of extraction methods the level of camphene could be decreased simultaneously [13].

Component discrimination of the EOs

In order to get more clear information regarding the differences and grouping of the two EOs components, chemometrics analysis, namely PCA and heatmap with dendrogram were carried out in this study. Chemometric analysis was successfully used to identify the presence of clustering between two EOs based on their components [27]. In this study, PCA and Heatmap with dendrogram confirmed the chemical profile differences of the two EOs which grouped the samples closely within one variety and separated them among two varieties. According to **Figure 2**, two discriminant clusters highlight the dissimilarity between them and 93.2% of the variability in the data is explained by PC1 (84.9%) and PC2 (8.3%). Finally, germacrene D and α-zingiberene are the key markers for differentiation between two ginger oils.

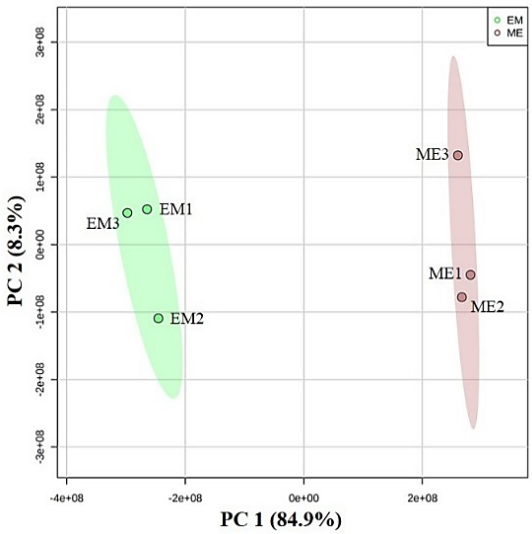

Figure 2. PCA Score plot analysis of emprit ginger (EM) and red ginger (ME) EOs

Heatmap with Euclidean distance measure and Ward clustering method (**Figure 3**) of major components demonstrated variations in the identifying compounds of two EOs. As illustrated in **Figure 3**, the blue color represents the lower content, while the red color represents the higher content. The heatmap with dendrogram clearly explains the distribution and abundance of each component in two EO between different varieties and within one variety. Emprit ginger (Em) appears to contain higher levels (marked in red) of sesquiterpene, such as α-zingiberene, and monoterpene, such as camphene. Meanwhile, red ginger (Me) contains higher levels of oxygenated monoterpenes, such as neral and geraniol. This result showed that heatmap with dendrogram is a powerful data visualization method for differentiation of two ginger EOs based on their components. Other studies have also demonstrated the use of chemometric to discrimination of the EO with different methods, geographic origins and the weather conditions [28,29].

Molecular docking studies

Molecular docking is an effective method for obtaining preliminary information before conducting research in a wet laboratory. We have used this method before to reveal the potential of Andaliman (*Zanthoxylum acanthopodium* DC.) fruit essential oil as an anti-aging agent and anti-acne potency of red ginger [30,31]. In this study, all identified components were further subjected to molecular docking study to confirm their potential to inhibit the skin-aging-related enzymes. For this purpose, collagenase (2TCL), hyaluronidase (2PE4), elastase (3F19) and tyrosinase (5M8R) were used as protein targets. Each enzyme has a role in the skin-aging process. Collagenase is an enzyme that breaks down and degrades collagen in the skin when activated. Elastase is responsible to break down and degrade elastin resulting in premature skin-aging, characterized by wrinkles and freckles. Collagen and elastin found in the skin with a major role in maintaining skin elasticity, flexibility, integrity, and sallowness. Apart from that, hyaluronidase also plays a role in skin aging by breaking down hyaluronic acid, causing the skin to lose strength, flexibility and moisture [9]. Meanwhile, tyrosinase plays a role in melanogenesis and enzymatic browning, inhibiting this enzyme to prevent or inhibit hyper-pigmentation and is used as a skin whitening agent [32]. Therefore, inhibition of these enzymes may be able to prevent or delay skin-aging.

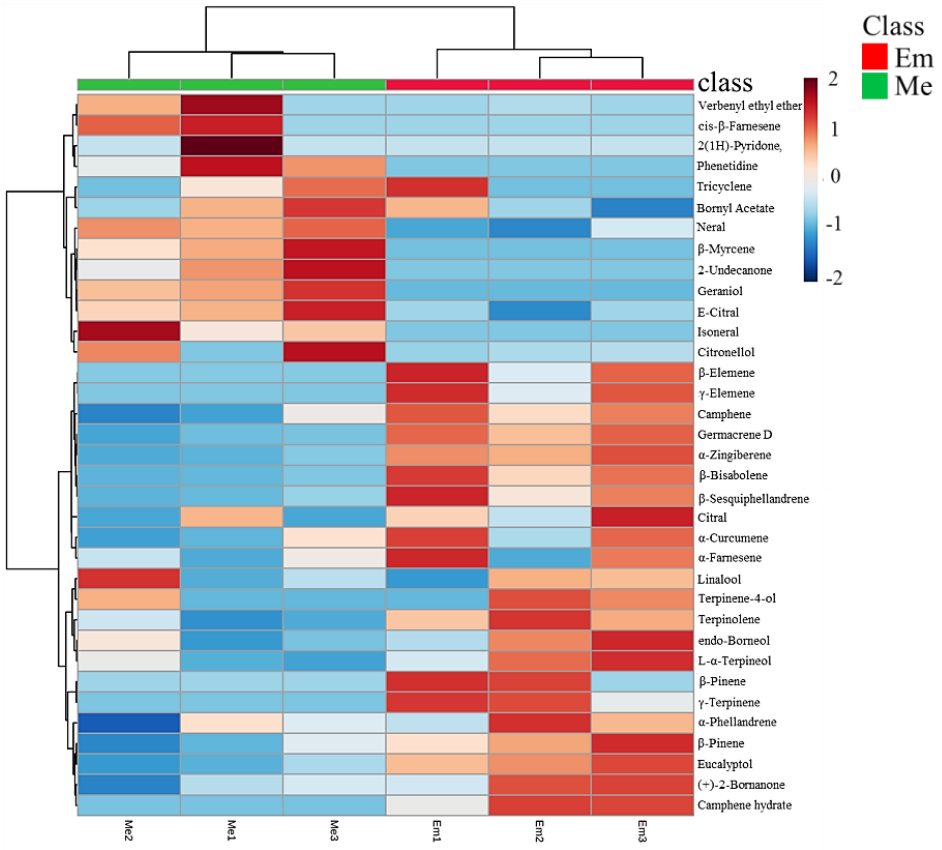

Figure 3. Heatmap with dendrogram of two ginger EOs components

Table 3. Binding free energy (*ΔG*) and inhibition constant (K_i) of the two Indonesian ginger EO components

Ligand	Hyaluronidase		Collagenase		Elastase		Tyrosinase	
	Free energy (kcal/mol)	K_i (μM)	Free energy (kcal/mol)	K_i (μM)	Free energy (kcal/mol)	K_i (μM)	Free energy (kcal/mol)	K_i (μM)
(-)-α-Pinene	-4.9	254	-5.8	55	-5.6	78	-5.5	92
Camphene	-5.1	181	-5.3	129	-5.4	109	-5.4	109
β-Myrcene	-5.8	55	-5.1	181	-5.9	47	-4.9	254
Eucalyptol	-5.3	129	-5.6	78	-6.1	33	-5.5	92
Linalool	-5.9	47	-5.6	78	-6.1	33	-4.8	300
Camphene hydrate	-5.1	181	-5.2	153	-5.8	55	-5.3	129
endo-Borneol	-4.9	254	-4.7	356	-5.8	55	-5.2	153
(+)-α-Terpineol	-6.0	40	-6.3	24	-7.0	7	-5.7	66
Citronellol	-5.3	129	-5.7	66	-6.1	33	-5.2	153
Neral	-5.8	55	-5.1	181	-5.9	47	-5.2	153
Geraniol	-5.6	78	-5.8	55	-6.3	24	-4.9	254
Citral	-6.1	33	-5.3	129	-6.4	20	-6.0	40
α-Curcumene	-7.0	7	-6.6	14	-8.2	1	-6.6	14
Germacrene D	-7.0	7	-6.1	33	-7.5	3	-7.0	7
α-Zingiberene	-7.1	6	-6.3	24	-7.8	2	-5.6	78
α-Farnesene	-6.6	14	-6.3	24	-7.4	4	-5.7	66
β-Bisabolene	-6.7	12	-6.6	14	-8.0	1	-6.2	28
β-Sesquiphellandrene	-6.8	10	-6.3	24	-7.9	2	-6.1	33
Ascorbic acid	-5.6	78	-6.4	20	-6.1	33	-6.0	40
ACT	-3.4	3199	-	-	-	-	-	-
RO4	-	-	-6.4	20	-	-	-	-
HS6	-	-	-	-	-7.6	3	-	-
MMS	-	-	-	-	-	-	-5.5	92

The results of the obtained docking scores are listed in **Table 3**, which shows some of the components have the potential to inhibit the enzymes tested. The preferred active component was the ligand with the lowest Gibbs free energy value (*ΔG*) and lowest inhibition constant (K_i). Some components, such as linalool, (+)-α-terpineol, geraniol, citral, germacrene D, α-zingiberene, α-farnesene, β-sesquiphellandrene, α-curcumene and β-bisabolene showed more higher affinity energy (more negative value) than ascorbic acid and native ligands of each tested enzymes as a control ligand for more than one enzymes. Based on their free energy, inhibition constant, and abundance, α-curcumene, α-zingiberene, β-bisabolene and β-sesquiphellandrene were components with more potential as anti-skin-aging agents. These components are mostly contained in emprit ginger EO. Therefore, EO from emprit ginger has more potential to be used as an anti-skin-aging agent compared to red ginger. Another study have also demonstrated the potential of ginger EO to protect the skin from UVB irradiation and photo-aging [14].

The docking simulation showed the binding affinity of α-curcumene was the highest compared to the others, except for the hyaluronidase and tyrosinase where α-zingiberene and germacrene D were the highest, respectively. **Figure 4A-D** shows 3D and 2D visualization of the interactions between best EO components and the amino acid residues of four studied enzymes. Meanwhile **Figure 4E-H** shows the 2D interaction of native ligands with each studied enzyme. The type of interactions between the EO components and enzymes were not hydrogen bond, but hydrophobic interactions such as van der Waals, pi-pi stacked and alkyl. **Figure 4A** shows the 2PE4–α-zingiberene complex involving 10 amino acid (AA) residues with van der Waals and alkyl interaction types, while the native ligand (ACT) was bounded to 2PE4 via 6 residues with more diverse types of interactions including van der Waals, conventional hydrogen bond and pi-anion (**Figure 4E**).

As shown in **Figure 4B**, the 2TCL–α-curcumene complex interacts via 12 AA residues with van der Waals, pi-anion, pi-pi stacked and alkyl interaction types. Meanwhile, the native ligand (RO4) forms a complex with 2TCL through interaction with 18 residues with the dominant type of interaction being conventional hydrogen bond and van der Waals (**Figure 4F**). In **Figure 4C** and **4G**, the number of residues involved in the formation of the 3F19–α-curcumene complex were more (12 AA) than 3F19-HS6 native ligand (5

AA). The interaction of van der Waals and alkyl dominates the 3F19–α-curcumene complex, while conventional hydrogen bonds are dominant in the 3F19–HS6 complex. **Figure 4D** & **4H** is a visualization of interaction for the 5M8R (tyrosinase). A total of 11 AA residues dominated by van der Waals interactions were involved in the formation of the 5M8R–germacrene D complex (**Figure 4D**), while 12 AA residues with the dominant interaction of van der Waals and conventional hydrogen bonds were involved in the MMS-5M8R complex (**Figure 4H**).

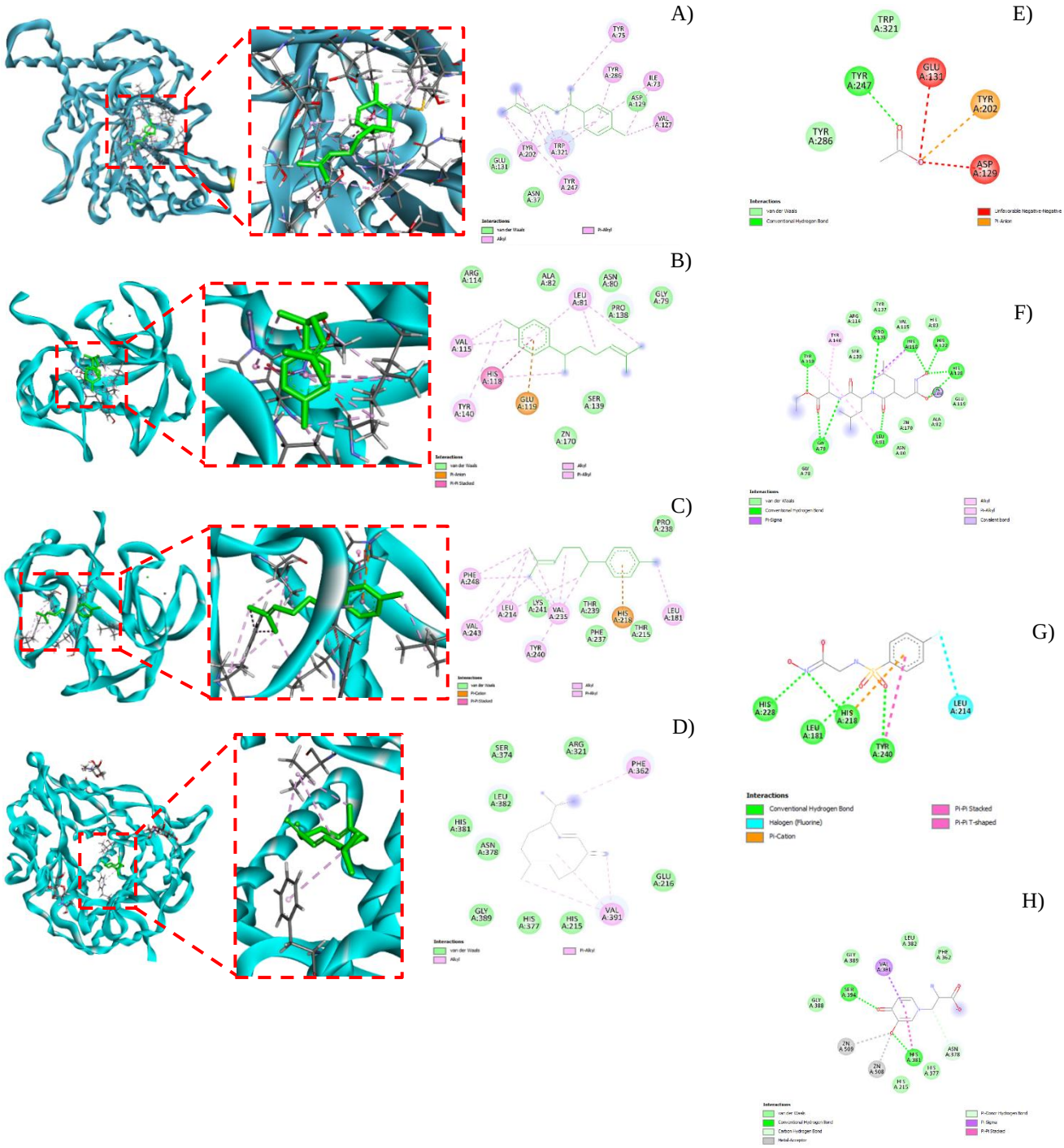

Figure 4. The 3D and 2D visualization interaction of (A) 2PE4–α-zingiberene; (B) 2TCL–α-curcumene; (C) 3F19–α-curcumene; (D) 5M8R–germacrene D; (E) 2PE4–ACT; (F) 2TCL–RO4; (G) 3F19–HS6; and (H) 5M8R–MMS

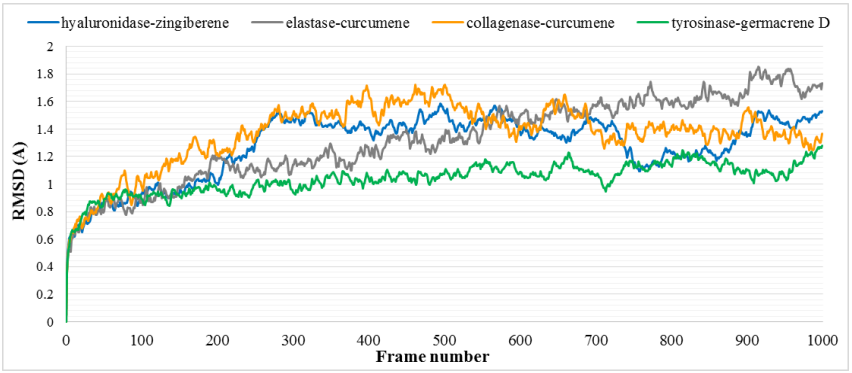

Figure 5. RMSD plots representing 1000 frames of MD simulation of 2PE4–α-zingiberene (blue line), 3F19–α-curcumene (gray line), 2TCL–α-curcumene (orange line), and 5M8R–germacrene D (green line) complexes

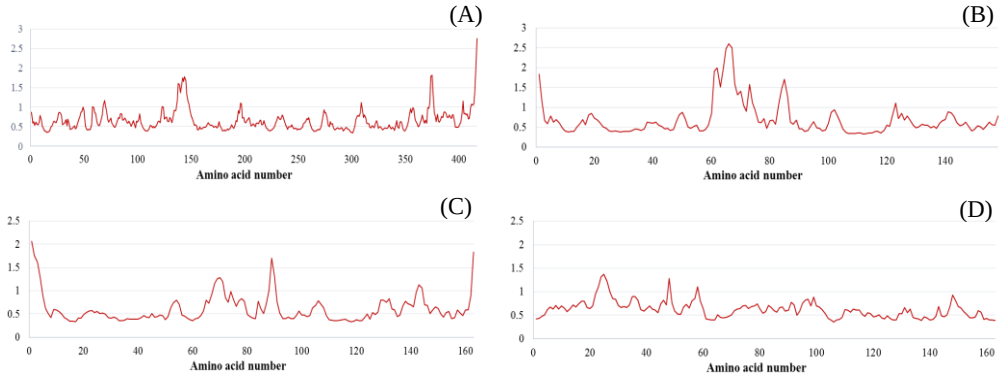

Figure 6. RMSF plots of (A) 2PE4–α-zingiberene; (B) 3F19–α-curcumene; (C) 2TCL–α-curcumene; (D) 5M8R–germacrene D complexes

Molecular dynamics trajectory stability

In order to obtain deeper information regarding how the four studied ligands interact with the active site of the proteins, stability interactions and the conformational changes in the complex, the analysis was continued with MD simulations. Four studied complexes, namely 2PE4–α-zingiberene, 3F19–α-curcumene, 5M8R–germacrene D and 2TCL–α-curcumene, were subjected to MD simulations. The average of RMSD value was used to evaluate each protein's structural changes. Changes in 3D protein structure are important to observe during simulation because related to their function. The higher average RMSD value indicates the increasingly unstable nature of the complex, as well as the mean value with an inclined fluctuation pattern.

The RMSD plots of the four studied complexes were shown in **Figure 5**. The average RMSD values of the 2PE4–α-zingiberene complex to be around 1.43 Å with the fluctuation range between 0.54–1.43 Å, this value is higher than other studied complexes. The 3F19–α-curcumene and 2TCL–α-curcumene complexes showed the average of RMSD 1.33 Å and 1.34 Å, respectively. However, the 3F19–α-curcumene plot continues to increase compared to 2PE4–α-zingiberene with a value range of 0–1.86 Å. Meanwhile 5M8R–germacrene D complexes showed average RMSD value 1.02 Å, with relatively more stable plot changes during simulation. Thus, the 5M8R–germacrene D complex is the most stable with the lowest average of RMSD value in the range of 0.8–1.4 and little plot changes. This result indicates studied ligands were accommodated in its binding site and there was no change in the three-dimensional structures of the proteins during simulation.

Fluctuations in the residual components

RMSF calculation was used to evaluate the effect of inhibitor binding on fluctuations and deviation in protein residues during MD simulation. The higher RMSF value indicates a relatively active interaction with the residues. **Figure 6** shows the fluctuations residue of the studied complexes. The calculated average RMSF values were 0.65 Å, 0.69 Å, 0.61 Å and 0.55 Å for 2PE4–α-zingiberene, 3F19–α-curcumene, 2TCL–α-curcumene and 5M8R–germacrene D complex systems, respectively. These results indicate that the 5M8R–germacrene D complex has the lowest residual fluctuation then others. Meanwhile a comparative analysis revealed 2PE4–α-

zingiberene complex have the highest number of fluctuated residues indicating relatively poor stability compared to the others.

The RMSF plots (**Figure 6**) revealed the stability of the interactions in each complex system during MD simulation. Each complex was relatively stable with a low RMSF value of the amino acid residues that were most influential in interactions with ligand, which was less than 1 Å. During MD simulation, the Asn37, Ile73, Tyr75, Val127, Asp129, Glu131, Tyr202, Tyr247, Tyr 286 and Trp321 were the most influential hyaluronidase amino acids in the interaction with α-zingiberene at the active site. Meanwhile, Leu181, Leu214, Thr215, His218, Val235, Phe237, Thr239, Tyr240, Lys241, Val243 and Phe248, were the elastase amino acids that are most influential in the interaction with α-curcumene. In collagenase, Gly79, Asn80, Leu81, Ala82, Arg114, Val115, His118, Glu119, Pro138, Ser139 and Tyr140, were the most influential amino acids in the interaction with α-curcumene. While His215, Phe362, Asn378, His381, Leu382, Gly389 and Val391, were the most influential amino acids in the interaction of the tyrosinase with germacrene D on the active site during the MD simulation.

Alterations in solvent accessibility

In order to evaluate the proportion of protein surface interacting with the solvent, such as water, SASA calculation was used. SASA was also used to predict the degree of complex conformational changes that occur during the binding process [33]. **Figure 7** was shown the variation of solvent accessibility each studied complexes during simulations. Based on the resulting plots pattern, the extent of the conformational changes during inhibitor binding simulation can be predicted. The resulting calculation showed the increasing SASA value of the all studied complex systems at the beginning of the simulation, which is then relatively steady. The increase in this value may indicate that the protein is unfolded during simulation [17]. The 5M8R–germacrene D has shown a relatively less extent, indicating more stability than the others.

ADMET Analysis

To determine the feasibility of emprit ginger EO components as an anti-skin-aging, ADMET characteristic and pharmacokinetics analysis was carried out with AdmetSAR against the four best components, namely α-zingiberene, α-curcumene, β-bisabolene and β-sesquiphellandrene, while ascorbic acid was used as the control. The ADMET properties play an important role in the development or discovery of new drugs [34]. AdmetSAR is a comprehensive open source and free tool for assessment of ADMET properties of a chemical [23]. This study has revealed studied components that have met the requirements of Lipinski's rule. The results of ADMET's pharmacokinetic analysis are listed in **Table 4**. As shown in **Table 4**, α-curcumene, β-bisabolene and β-sesquiphellandrene have the potential to cause eye irritation. All the analyzed components also have the potential to cause skin sensitization. Meanwhile, the bioavailability of the components was stated to be good. The levels of mutagenesis and carcinogenicity of the components were declared safe, not carcinogenic, and not mutagenic. Although this study shows the potential of emprit ginger EO as anti-skin-aging, in vivo test must be carried out to observe its effects on living cells.

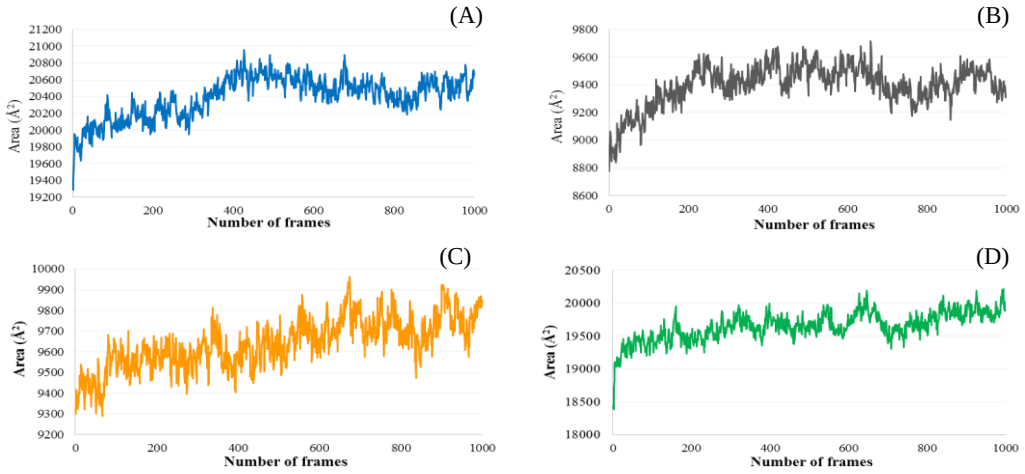

Figure 7. SASA plots of (A) 2PE4–α-zingiberene; (B) 3F19–α-curcumene; (C) 2TCL–α-curcumene; (D) 5M8R–germacrene D complexes

Table 4. AdmetSAR analysis of the four most potential components in *Z. officinale* var *amarum* EO

	ADMET Value				
	ZGB	CCM	BSB	BSP	ASA
Physicochemical properties					
Molecular weight	204.36	202.34	204.36	204.36	176.12
Hydrogen bond donors	0	0	0	0	4
Hydrogen bond acceptors	0	0	0	0	6
Log P	4.89	4.84	5.04	4.89	-1.41
Rotatable bonds	4	4	4	4	2
ADMET Predicted profile					
Absorption					
Human intestinal absorption	+	+	+	+	+
Caco-2 permeability	+	+	+	+	-
Blood-brain barrier	+	+	+	+	+
P-glycoprotein inhibitor	-	-	-	-	-
P-glycoprotein substrate	-	-	-	-	-
Distribution					
Subcellular localization	Lysosomes	Nucleus	Lysosomes	Lysosomes	Mitochondria
Metabolism					
OATP2B1 inhibitor	-	-	-	-	-
OATP1B1 inhibitor	+	+	+	+	+
OATP1B3 inhibitor	+	+	+	+	+
CYP450 3A4 substrate	-	-	-	-	-
CYP450 2C9 substrate	-	-	-	-	-
CYP450 2D6 substrate	-	-	-	-	-
CYP450 3A4 inhibition	-	-	-	-	-
CYP450 2C9 inhibition	-	-	-	-	-
CYP450 2C19 inhibition	-	-	-	-	-
CYP450 2D6 inhibition	-	-	-	-	-
CYP450 1A2 inhibition	-	-	-	-	-
CYP inhibitory promiscuity	-	+	-	-	-
Excretion - Toxicity					
Human oral bioavailability	-	+	+	+	+
Carcinogenicity (binary)	-	-	-	-	-
Eye irritation	-	+	+	+	-
AMES mutagenesis	-	-	-	-	-
Human ether-a-go-go-related gene inhibition	+	+	-	+	-
Skin sensitization	+	+	+	+	-
Respiratory toxicity	+	-	-	+	-
Estrogen receptor binding	-	-	-	-	-
Androgen receptor binding	-	-	-	-	-
Thyroid receptor binding	-	-	-	-	-
Glucocorticoid receptor binding	-	-	-	-	-
Enzyme inhibition	0.29	-0.14	0.27	0.27	0.20

Note: ZGB= α-zingiberene, CCM= α-curcumene, BSB= β-bisabolene, BSP= β-sesquiphellandrene, ASA= ascorbic acid, "+" = Yes, "-"= No.

4. CONCLUSIONS

This study successfully revealed the differences in the components of emprit (*Z. officinale* var *amarum*) and red ginger (*Z. officinale* var *rubrum*) EOs. Eucalyptol (17.92%) and camphene (15.12%) were the most abundant in emprit and red ginger EOs, respectively. Chemometric analysis showed the chemical variability and the interrelationships between the two EOs, while germacrene D and α-zingiberene are the key markers for their differentiation. Docking and MD simulations followed by ADMET analysis have shown the four components that are more abundant in emprit ginger EO, namely α-curcumene, α-zingiberene, β-bisabolene and β-sesquiphellandrene, have the best docking score, relatively stable interaction with the studied enzymes, declared safe and have the most potential as anti-aging agents. Therefore, the EO of emprit

ginger represents promising sources of anti-skin-aging for further research.

ACKNOWLEDGMENTS

This work was supported by the Directorate General of Higher Education, Research and Technology, Ministry of Education, Culture and Technology of the Republic of Indonesia, with funding number: 001/E5/PG.02.00PT/2022, to The Research and Community Service Institute, IPB University. This work was partially supported by the United Graduate School of Agricultural Sciences-Gifu University (UGSAS-GU) through UGSAS-GU Lab station at IPB University.

REFERENCES

1. Supu R, Diantini A, Levita J. Red ginger (Zingiber officinale var. rubrum): its chemical constituents, pharmacological activities and safety. *FITOFARMAKA J Ilm Farm*. 2019;8:23-29. doi:10.33751/jf.v8i1.1168

2. Höferl M, Stoilova I, Wanner J, et al. Composition and comprehensive antioxidant activity of ginger (Zingiber officinale) essential oil from Ecuador. *Nat Prod Commun*. 2015;10(6):1085-1090. doi:10.1177/1934578X1501000672

3. Apak R, Özyürek M, Güçlu K, Çapanoğlu E. Antioxidant activity/capacity measurement. 1. classification, physicochemical principles, mechanisms, and electron transfer (ET)-based assays. *J Agric Food Chem*. 2016;64(5):997-1027. doi:10.1021/acs.jafc.5b04739

4. Chaudhary M, Khan A, Gupta M. Skin ageing: pathophysiology and current market treatment approaches. *Curr Aging Sci*. 2020;13(1):22-30. doi:10.2174/1567205016666190809161115

5. Zhang S, Duan E. Fighting against skin aging: the way from bench to bedside. *Cell Transplant*. 2018;27(5):729-738. doi:10.1177/0963689717725755

6. Lee H, Hong Y, Kim M. Structural and functional changes and possible molecular mechanisms in aged skin. *Int J Mol Sci*. 2021;22(22):12489. doi:10.3390/ijms222212489

7. Ansary TM, Hossain MR, Kamiya K, Komine M, Ohtsuki M. Inflammatory molecules associated with ultraviolet radiation-mediated skin aging. *Int J Mol Sci*. 2021;22(8):3974. doi:10.3390/ijms22083974

8. Lee EJ, Kim JY, Oh SH. Advanced glycation end products (AGEs) promote melanogenesis through receptor for AGEs. *Sci Rep*. 2016;6:27848. doi:10.1038/srep27848

9. Jiratchayamaethasakul C, Ding Y, Hwang O, et al. In vitro screening of elastase, collagenase, hyaluronidase, and tyrosinase inhibitory and antioxidant activities of 22 halophyte plant extracts for novel cosmeceuticals. *Fish Aquat Sci*. 2020;23(6):1-9. doi:10.1186/s41240-020-00149-8

10. Younis MM, Ayoub IM, Mostafa NM, et al. GC/MS profiling, anti-collagenase, anti-elastase, anti-tyrosinase and anti-hyaluronidase activities of a Stenocarpus sinuatus leaves extract. *Plants*. 2022;11(7):1-19. doi:10.3390/plants11070918

11. Anwar S, Almatroudi A, Allemailem KS, Joseph RJ, Khan AA, Rahmani AH. Protective effects of ginger extract against glycation and oxidative stress-induced health complications: an in vitro study. *Processes*. 2020;8(4):1-20. doi:10.3390/pr8040468

12. Sahardi NFNM, Makpol S. Ginger (Zingiber officinale Roscoe) in the prevention of ageing and degenerative diseases: review of current evidence. *Evid Based Complement Altern Med*. 2019;2019:5054395. doi:10.1155/2019/5054395

13. Batubara I, Badrunanto, Wahyuni WT, Farid M. Combination of extraction and distillation red ginger rhizome on the composition of active compounds and tyrosinase inhibitory activity. *IJASEIT*. 2023;13(2):431-437. doi:10.18517/ijaseit.13.2.17606

14. Feng J, Du Z, Zhang L, et al. Chemical composition and skin protective effects of essential oil obtained from ginger (Zingiber officinale Roscoe). *J Essent Oil Bear Pl*. 2018;21(6):1542-1549. doi:10.1080/0972060X.2018.1533436

15. Asoka SF, Batubara I, Lestari AR, Wahyuni WT. Compounds in Indonesian ginger rhizome extracts and their potential for anti-skin aging based on molecular docking. *Cosmetics*. 2022;9(6):128. doi:doi:10.3390/cosmetics9060128

16. Catinella G, Badalamenti N, Ilardi V, Rosselli S, De Martino L, Bruno M. The essential oil compositions of three Teucrium taxa growing wild in Sicily: HCA and PCA analyses. *Molecules*. 2021;26(3):1-19. doi:10.3390/molecules26030643

17. Gyebi GA, Ogunyemi OM, Ibrahim IM, et al. Inhibitory potentials of phytocompounds from Ocimum gratissimum against anti-apoptotic BCL-2 proteins associated with cancer: an integrated computational study. *Egypt J Basic Appl Sci*. 2022;9(1):588-608. doi:10.1080/2314808X.2022.2106095

18. Trott O, Olson AJ. AutoDock Vina: improving the speed and accuracy of docking with a new scoring function, efficient optimization, and multithreading. *J Comput Chem*. 2010;31(2): 455-461. doi:10.1002/jcc.21334

19. Jack KS, Razip M, Bhawani SA. Pharmacophore study, molecular docking and molecular dynamic simulation of virgin coconut oil derivatives as anti-inflammatory agent against COX-2. *Chem Biol Technol Agric*. 2022;9(1):73. doi:10.1186/s40538-022-00340-0

20. Phillips JC, Braun R, Wang W, et al. Scalable, molecular dynamics with NAMD. *J Comput Chem*. 2005;26(16):1781-1802. doi:10.1002/jcc.20289

21. Lee J, Cheng X, Swails JM, et al. CHARMM-GUI input generator for NAMD, GROMACS, AMBER, OpenMM, and CHARMM/OpenMM simulations using the CHARMM36 additive force field. *J Chem Theory Comput*. 2016;12(1):405-413. doi:10.1021/acs.jctc.5b00935

22. Humphrey W, Dalke A, Schulten K. VMD: visual molecular dynamics. *J Mol Graph*. 1996;14(1):33-38. doi:10.1016/0263-7855(96)00018-5

23. Cheng F, Li W, Zhou Y, et al. AdmetSAR: a comprehensive source and free tool for assessment of chemical ADMET properties. *J Chem Inf Model*. 2012;52(11):3099-3105. doi:10.1021/ci300367a

24. Jayasundara NDB, Arampath P. Effect of variety, location & maturity stage at harvesting, on essential oil chemical composition, and weight yield of Zingiber officinale roscoe grown in Sri Lanka. *Heliyon*. 2021;7(3):e06560. doi:10.1016/j.heliyon.2021.e06560

25. Nissa A, Utami R, Sari AM, Nursiwi A. Combination effect of nisin and red ginger essential oil (Zingiber officinale var. rubrum) against foodborne pathogens and food spoilage microorganisms. In: *AIP Conf. Proc.* Vol 2014. ; 2018:020023. doi:10.1063/1.5054427

26. Rinanda T, Isnanda RP, Zulfitri. Chemical analysis of red ginger (Zingiber officinale Roscoe var rubrum) essential oil and its anti-biofilm activity against Candida albicans. *Nat Prod Commun*. 2018;13(12):1587-1590. doi:10.1177/1934578X1801301206

27. El-Din MIG, Youssef FS, Altyar AE, Ashour ML. GC/MS analyses of the essential oils obtained from different Jatropha species, their discrimination using chemometric analysis and assessment of their antibacterial and anti-biofilm activities. *Plants*. 2022;11(1268):1-18. doi:10.3390/plants11091268

28. Acimovic M, Loncar B, Pezo M, et al. Volatile compounds of Nepeta nuda L. from Rtanj mountain (Serbia). *horticulturae*. 2022;8(2):85. doi:10.3390/horticulturae8020085

29. Pan X, Li H, Chen D, et al. Comparison of essential oils of Houttuynia cordata Thunb. from different processing methods and harvest seasons based on GC-MS and chemometric analysis. *Int J Anal Chem*. 2021;Vol. 2021:Article ID 8324169. doi:10.1155/2021/8324169

30. Kintamani E, Batubara I, Kusmana C, Tiryana T, Mirmanto E, Asoka SF. Essential oil compounds of andaliman (Zanthoxylum acanthopodium DC.) fruit varieties and their utilization as skin anti-aging using molecular docking. *Life*. 2023;13(3):754. doi:10.3390/life13030754

31. Wahyudi ST, Wahyuni W, Asoka S, Batubara I. Gingerol and shogaol content of Zingiber officinale var. rubrum and its potency as anti acnes based on in silico study. *AIP Conf Proc*. 2022;2553:20037. doi:10.1063/5.0103689

32. Zolghadri S, Bahrami A, Khan MTH, et al. A comprehensive review on tyrosinase inhibitors. *J Enzym Inhib Med Chem*. 2019;34(1):279-309. doi:10.1080/14756366.2018.1545767

33. Shahbaaz M, Nkaule A, Christoffels A. Designing novel possible kinase inhibitor derivatives as therapeutics against Mycobacterium tuberculosis: an in silico study. *Sci Rep*. 2019;9:4405. doi:10.1038/s41598-019-40621-7

34. Abdullahi SH, Uzairu A, Shallangwa GA, Uba S, Umar AB. Molecular docking, ADMET and pharmacokinetic properties predictions of some di-aryl pyridinamine derivatives as estrogen receptor (Er+) kinase inhibitors. *Egypt J Basic Appl Sci*. 2022;9(1):180-204. doi:10.1080/2314808X.2022.2050115.